Journal of the Korean Ceramic Society (2023) 60:896–904
https://doi.org/10.1007/s43207-023-00318-0

ORIGINAL ARTICLE

Effect of Zn-doping CdTe on the internal and external quantum efficiency: ab initio calculations

G. Kadim[1] · R. Masrour[1]

Received: 3 November 2022 / Revised: 9 June 2023 / Accepted: 5 July 2023 / Published online: 31 July 2023

Abstract
The photovoltaic properties depend on the internal (IQE) and external (EQE) quantum efficiency. However, to calculate this quantum efficiency theoretically, we have determined the optical and electronic properties of $Cd_{1-x}Zn_xTe$ bulk and CdTe thin film. CdTe thin film is immensely interesting narrow band gap semiconductor with high absorption 100×10^4 cm^{-1} for the visible solar spectrum having promising applications in new-generation electronics and photo-electronic devices. $Cd_{1-x}Zn_xTe$ bulk is a semiconductor with a narrow bandgap value. The band gap values decrease slightly linearly from 1.708 to 1.642 eV with increase of Zn content. Optical reflectivity and absorption are discussed in detail. The IQE and EQE quantum efficiency of CdTe thin film and Zn doping CdTe bulk are investigated and analyzed. Our results are more consistent with the experimental results.

Keywords Density functional theory · EQE · IQE · Zn-doping · CdTe thin film

1 Introduction

Photovoltaic is environmentally friendly [1, 2]. In fact, the photovoltaic properties depend on the internal (IQE) and external (EQE) quantum efficiency [3–6]. Theoretically, the quantum efficiency is related by determination of the optical properties [7–9]. Specifically, IQE is the ratio of the number of electronic charges collected to the number of photons absorbed. It makes it possible to overcome the reflectance and the transmittance of the cell. It only takes into account the absorbed photons [10, 11]. It means that the 1-R factor is always less than 1. This explains that the IQE is always bigger than the EQE [12, 13]. However, when the IQE is low, the active layer of the solar cell is not able to take advantage of all the photons [14].

Currently, the CdTe thin-film solar cell technology is widely produced in the world [15, 16]. This is because CdTe is chemically stable [17] and has distinct properties i.e. it has a direct band gap close to 1.5 eV, just in the middle of the solar spectrum, and possess high-absorption coefficient (α) ($> 10^4$ cm^{-1}) for the visible solar spectrum [18, 19]. The EQE of CdTe thin film remarkable electron photon of about 92% and short circuit with current density greater than 25 (mA/Cm^2) [20]. With regard to the open circuit voltage of the CdTe it breaks the 1 V barrier [21].

On the other hand, CdTe can be easily doped with either p-type or n-type semiconductors. Furthermore, in the periodic table. We find that the elements in the first and fifth columns act as acceptors, while the elements in the third and seventh columns act as donors. Moreover, some of these elements show a particular behavior in CdTe, depending on their place(s) in the crystal lattice.

Recently, work intensively obtained high-class CdZnTe crystals at a low cost. Due to their working potential at room temperature. Since it works at room temperature, it is also very important for nuclear detectors [22, 23].

In this work we will study the effect of Zn-doping CdTe bulk on external EQE and internal IQE quantum efficiency using FP-LAPW method and to compare the results obtained with the experimental results.

✉ R. Masrour
rachidmasrour@hotmail.com

[1] Laboratory of Solid Physics, Faculty of Sciences Dhar El Mahraz, Sidi Mohamed Ben Abdellah University, BP 1796, Fez, Morocco

2 Computational detail

The DFT calculation implemented on Wien2k package employed to calculate the electronic and optical properties of $Cd_{1-x}Zn_xTe$ ($0<x<0.5$) bulk and CdTe thin film. The lattice parameter of CdTe is $a=6.529$ Å (Fig. 1) [24]. GGA-PBE is used to describe the electron–electron exchange and correlation potential. While TB-mBJ approximation is used to ameliorate the gap's energy [25–27].

The modified Becke–Johnson (mBJ) potential read as:

$$U_{\chi,\sigma}^{\mathrm{mBJ}}(r) = cU_{\chi,\sigma}^{\mathrm{BR}}(r) + (3c-2)\frac{1}{\pi}\sqrt{\frac{5}{12}}\sqrt{\frac{2t_\sigma(r)}{\rho_\sigma(r)}}. \quad (1)$$

Or $\rho(r) = \sum_{i=1}^{n_\sigma} \left|\psi_{i,\sigma}(r)\right|^2$ is the density of electrons, $t_\sigma(r) = \frac{1}{2}\sum_{i=1}^{n_\sigma} \nabla\psi_{i,\sigma}^*(r)\nabla\psi_{i,\sigma}(r)$ is the kinetic energy density and $U_{\chi,\sigma}^{\mathrm{BR}}(r) = -\frac{1}{b_\sigma(r)}\left(1-\mathrm{e}^{-x_\sigma(r)} - \frac{1}{2}x_\sigma(r)\mathrm{e}^{-x_\sigma(r)}\right)$ is the potential of Becke–Roussel (BR) [26].

The cut off energy is −9.0 Ry. The full Brillouin zone is defined with 10×10×10 meshesof Monkhorst–Pack k points. The electronic states $4d^{10}\,5s^2$, $3d^{10}\,4s^2$ and $4d^{10}\,5s^2\,5p^4$ are considered as the valence states of Cd, Zn and Te atoms respectively.

The absorption and reflectivity are calculated from the dielectric function [28]:

$$\varepsilon(\omega) = \varepsilon_1(\omega) + \mathrm{i}\varepsilon_2(\omega) \quad (3)$$

With $\varepsilon_1(\omega)$ is the real part and $\varepsilon_2(\omega)$ the imaginary part

The EQE is given by:

$$\mathrm{EQE}(\lambda) = (1-R(\lambda))\left(1-N\mathrm{e}^{-\alpha(\lambda)}\right) \quad (3)$$

where $R(\lambda) = \left|\frac{\sqrt{\varepsilon(\lambda)}-1}{\sqrt{\varepsilon(\lambda)}+1}\right|^2$ and $\alpha(\lambda) = \frac{\sqrt{2}}{c}\lambda\sqrt{-\varepsilon_1(\lambda)+\sqrt{\varepsilon_1(\lambda)^2+\varepsilon_2(\lambda)^2}}$ are reflectivity and absorption respectively. N is the number of layers in the thin film structure. It's $N=1$ if the structure is bulk.

The internal quantum efficiency (IQE) is given by:

$$\mathrm{IQE} = \frac{\mathrm{EQE}}{1-R}. \quad (4)$$

3 Discussion and results

3.1 Electronic properties

Studying electronic properties of materials gives us an idea of all physical properties of these materials. These properties are manifested in the total and partial electron density.

The calculated density of states (DOS) of our materials is discussed in terms of the contribution of the constituent atoms various s, p, and d-states. The Fermi level is marked with dashed lines, which are located at point zero.

3.1.1 CdTe thin film

The total and partial density of CdTe thin film plotted in Fig. 2. Figure 2a shows that CdTe is a semiconductor with a narrow band gap 1.58 eV using TB-mBJ. This value in good agreement with the value found theoretically by LDA + U

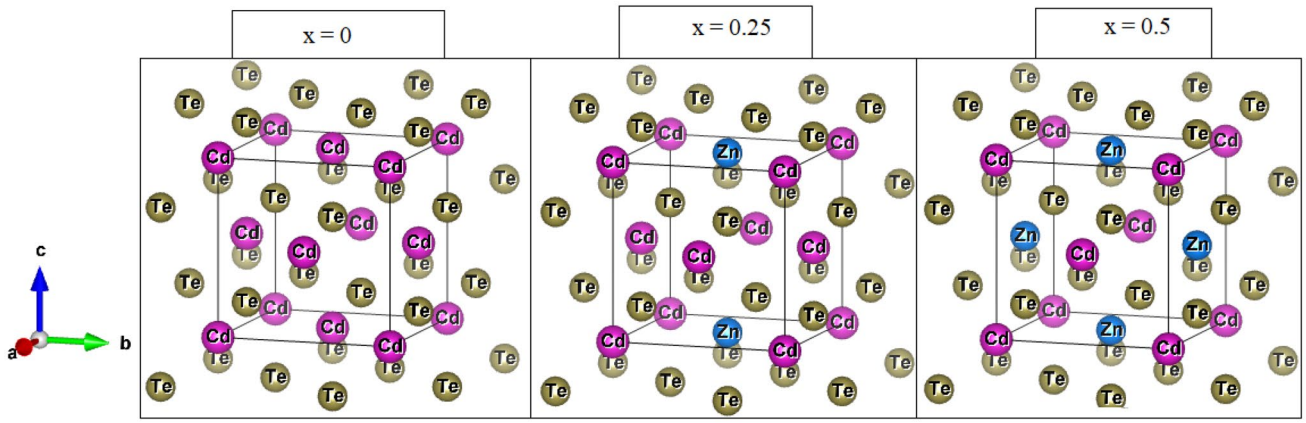

Fig. 1 Structure of Zn-doped CdTe

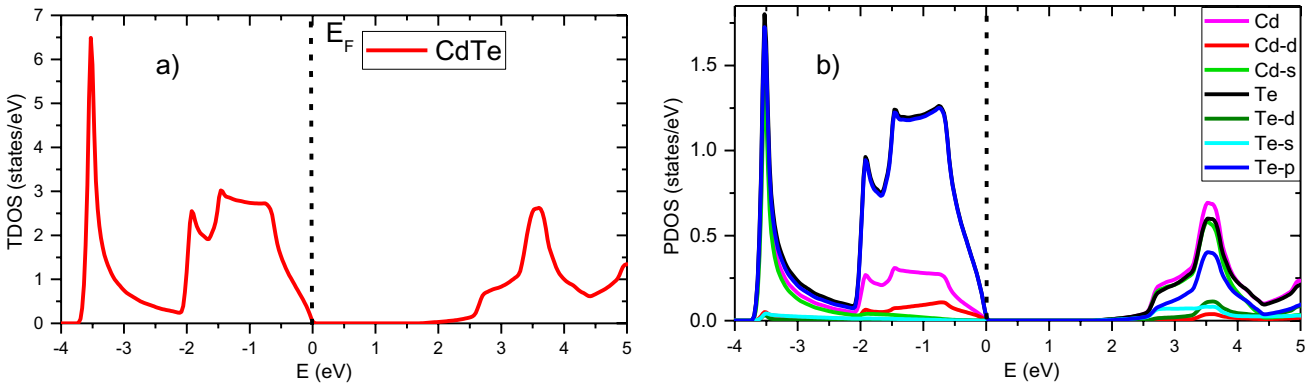

Fig. 2 TDOS (**a**) and PDOS (**b**) of CdTe thin film using TB-mBJ approximation

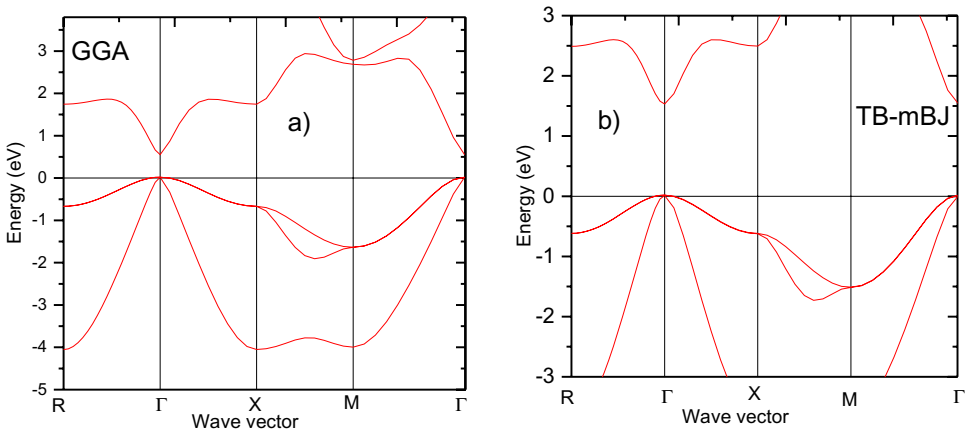

Fig. 3 Energy band structure calculated using GGA (**a**) and TB-mBJ (**b**) approximations of CdTe thin film

(1.53 eV) [24] and experimentally value (1.5 eV) [29]. As shown in Fig. 2b, the Te-p and Cd-d orbitals are often responsible for this band gap. In Fig. 3 we plotted the band structure of CdTe thin film. This figure demonstrate that the CdTe thin film has direct band gap (Γ–Γ) property. This property makes CdTe thin films suitable for single-junction solar cells and ideal for photovoltaic applications [30].

3.1.2 $Cd_{1-x}Zn_xTe$ ($0 < x < 0.5$) bulk

The total (TDOS) and partial (PDOS) density of $Cd_{1-x}Zn_xTe$ bulk are plotted in Fig. 4a and b. Figure 4a shows that $Cd_{1-x}Zn_xTe$ bulk have semiconductor character with a narrow band gap 1.708, 1.673 and 1.642 eV for $x = 0$, 0.25 and 0.5 using TB-mBJ approximation. Figure 4a shows the dependence of the change in the bandgap value on the change in the zinc content in $Cd_{1-x}Zn_xTe$ bulk. The bandgap value decreases linearly from 1.708 to 1.642 eV using TB-mBJ when substituted Zn in Cd [31], which may be due to the quantum nature of $Cd_{1-x}Zn_xTe$ bulk. THIS may be due to the quantum nature of these systems A new energy levels appear in the positive energy region [3.34 eV, 3.67 eV] due to Zn atom, which are absent in the band diagram of pure cadmium telluride.

3.2 Internal and external quantum efficiency

The calculation of the external and internal quantum efficiency and photovoltaic properties linked by the calculation of absorption and reflectivity.

3.2.1 CdTe thin film

The absorption curve of CdTe thin film is presented in Fig. 5a). The three peaks correspond to a direct (Γ–Γ) transition. The direct optical transition mainly goes from the occupied state of the valence band (VB) Te-*p* and Cd-*d*. The transition band 3–4 eV ranges between the Te-*p*, Cd-*s* in valance band and Te-*p* Te-*s*, Te-*d*, Cd-*d* and Cd-*s*. The transition band 5–6 eV ranges between the Te–*d* state and the Te-*p* state in the conduction band. Band transitions from 6 to 8 V come from the Te–*s* state, Te-*p* and the Cd-*d* in valence band and Te-*p* Te-*d* states in the conduction band.

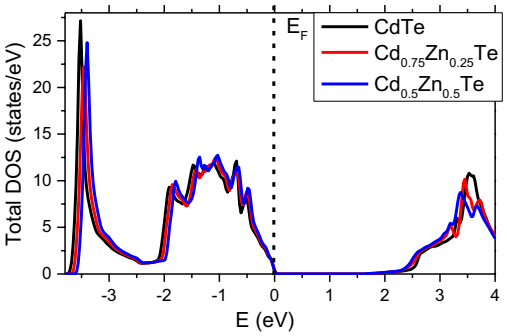

a Total DOS of Zn-doping CdTe using TB-mBJ approximation

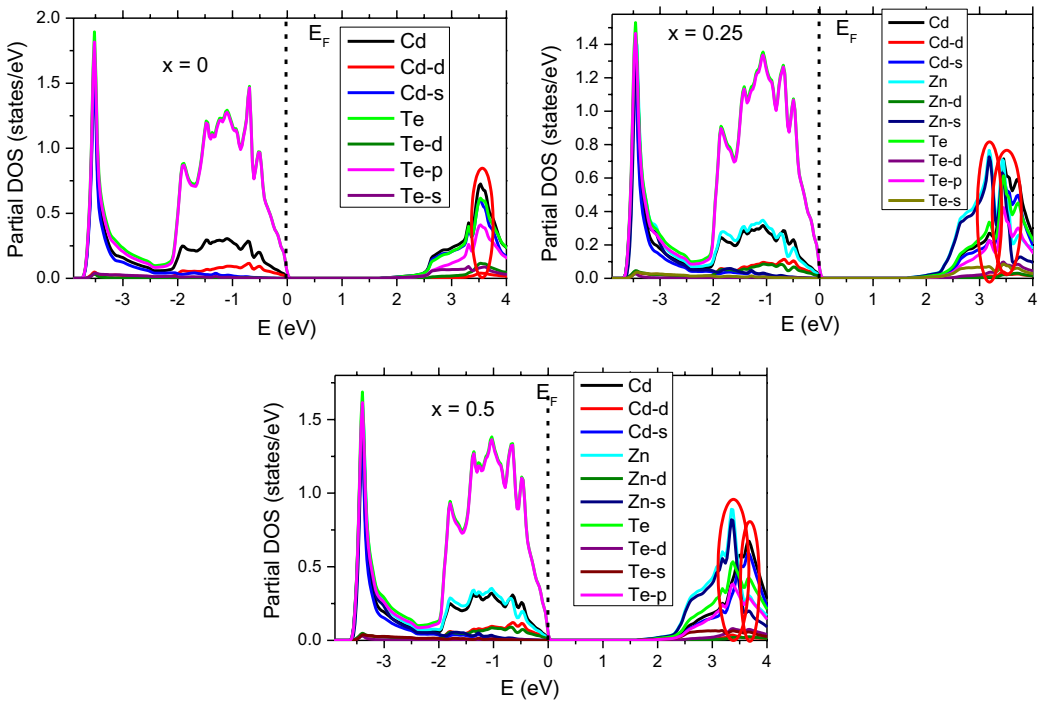

b Partial DOS of Zn-doping CdTe using TB-mBJ approximation

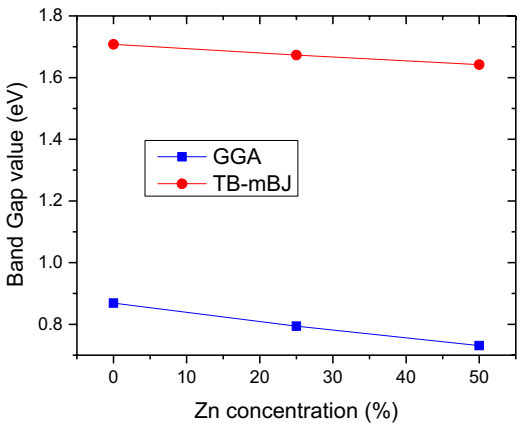

c Band Gap value of Zn doping CdTe bulk using GGA (a) and TB-mBJ (b) approximation

Fig.4 **a** Total DOS of Zn-doping CdTe using TB-mBJ approximation. **b** Partial DOS of Zn-doping CdTe using TB-mBJ approximation. **c** Band gap value of Zn doping CdTe bulk using GGA (blue) and TB-mBJ (red) approximations

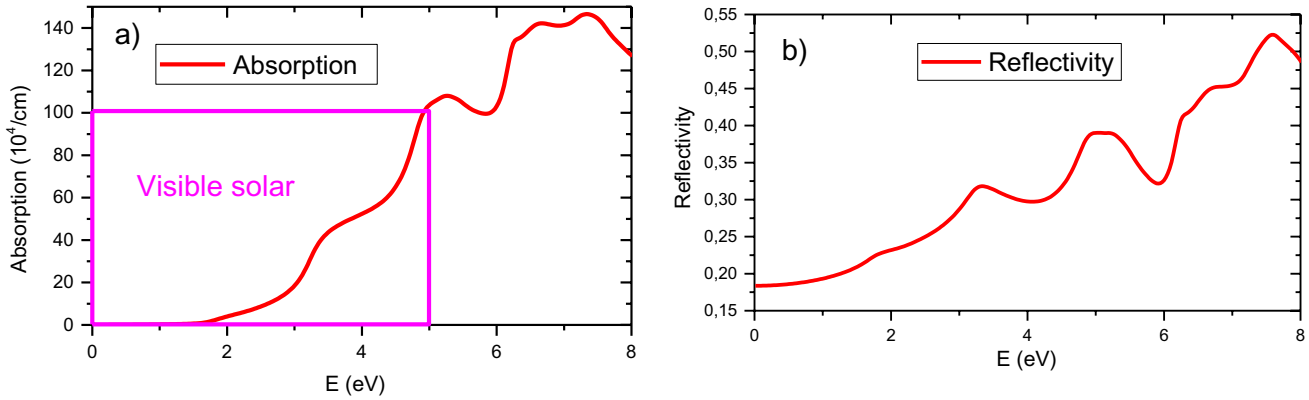

Fig. 5 Absorption (**a**) and reflectivity (**b**) of CdTe thin film vs. of photon energy

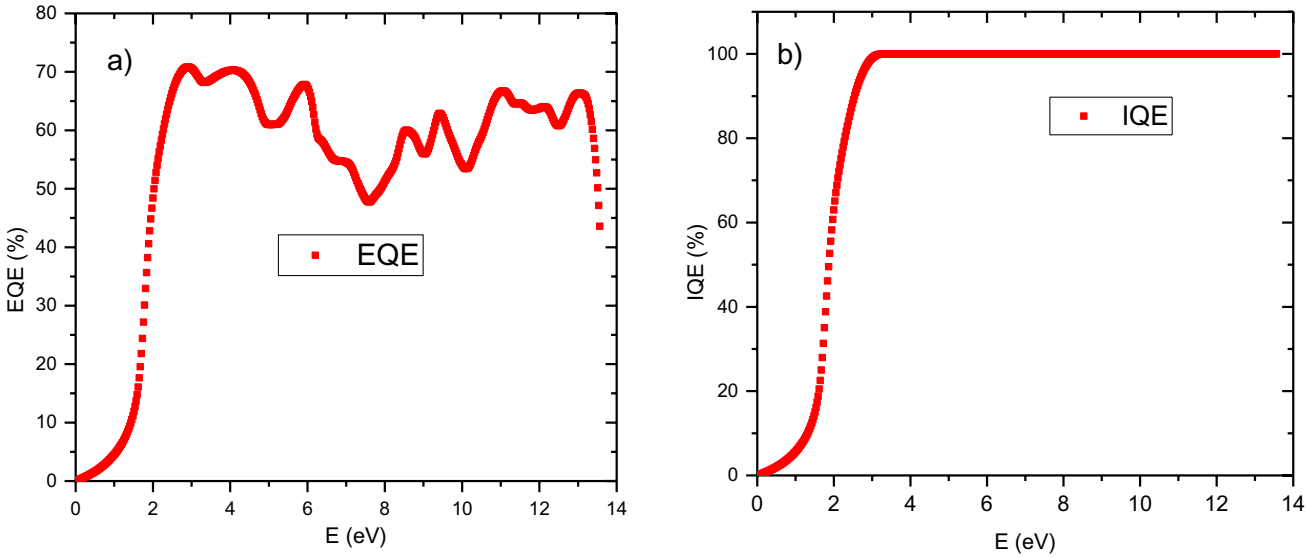

Fig. 6 EQE (**a**) IQE (**b**) vs. of photon energy for CdTe thin film

However, the reflectivity of CdTe display in Fig. 5b. It has starts at 0.184%. Several peaks are seen in the reflectivity plot which is due to electron transition.

Figure 6a displays the external quantum efficiency EQE for CdTe thin film. The maximum of EQE for CdTe is equal to 72.55% above band gap 1.58 eV. This value very close to that found experimentally 80% [32] and 92% [20]. Regarding Fig. 6b the maximum internal quantum efficiency of CdTe thin film was above 100% when the light energy is larger than the band gap 1.58 eV. This value of IQE demonstrates efficient conversion of absorbed photons into electrons and shows that efficient transport of these carriers out of the apparatus [33].

3.2.2 $Cd_{1-x}Zn_xTe$ ($0 < x < 0.5$) bulk

The absorption curve of $Cd_{1-x}Zn_xTe$ bulk is presented in Fig. 7a. The first peak mainly starts from the occupied state of the valence band (VB) Te-*p* and Cd-*d* for CdTe and Te-*p*, Zn-*d* and Cd-*d* for Zn doping CdTe. The transition band 3–4 eV ranges between the Te-*p*, Cd-*s* in valance band and Te-*p* Te-*s*, Te-*d*, Cd-*d* and Cd-*s* in conduction band. While when Zn doped Cd, this peak also goes from Zn-*s* in valence band and conduction band. In addition, the absorption spectra show that with an increase in the Zn concentration, the absorption edges shift towards shorter waves. In addition, there is a high absorption of the $Cd_{1-x}Zn_xTe$ materials under

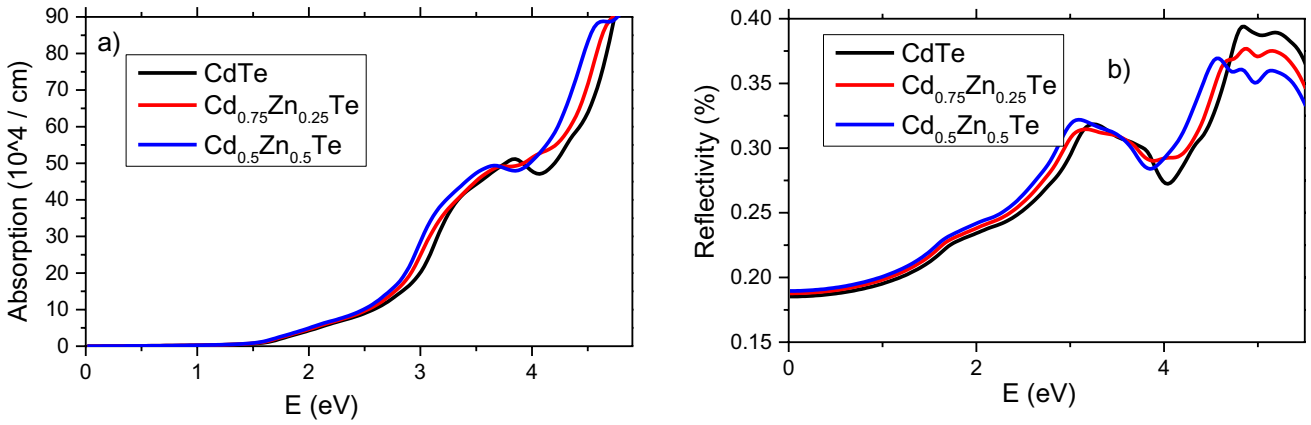

Fig. 7 Absorption (**a**) and reflectivity (**b**) of Zn-doping CdTe bulk vs. of photon energy

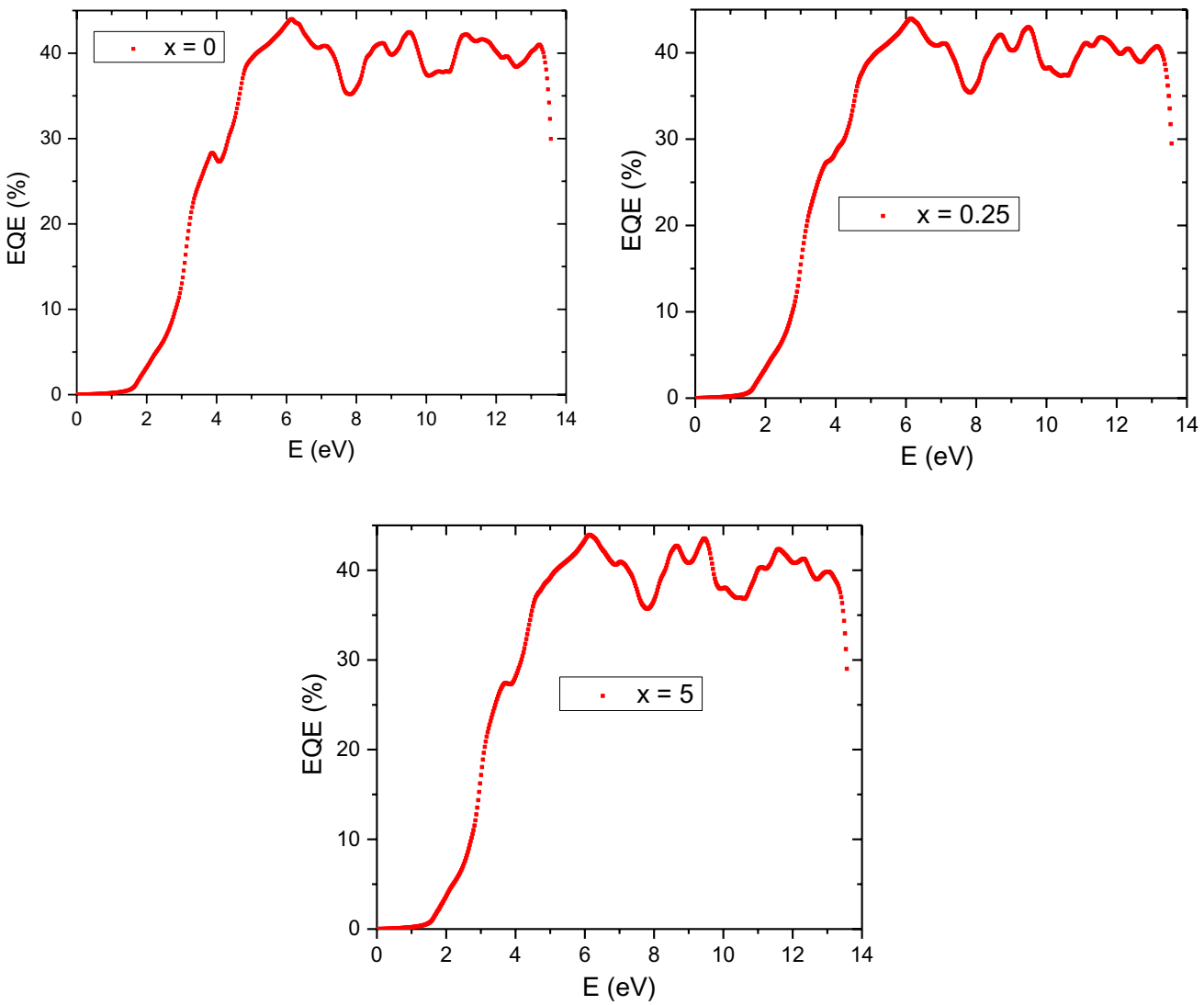

Fig. 8 External quantum efficiency of Zn-doping CdTe bulk vs. of photon energy

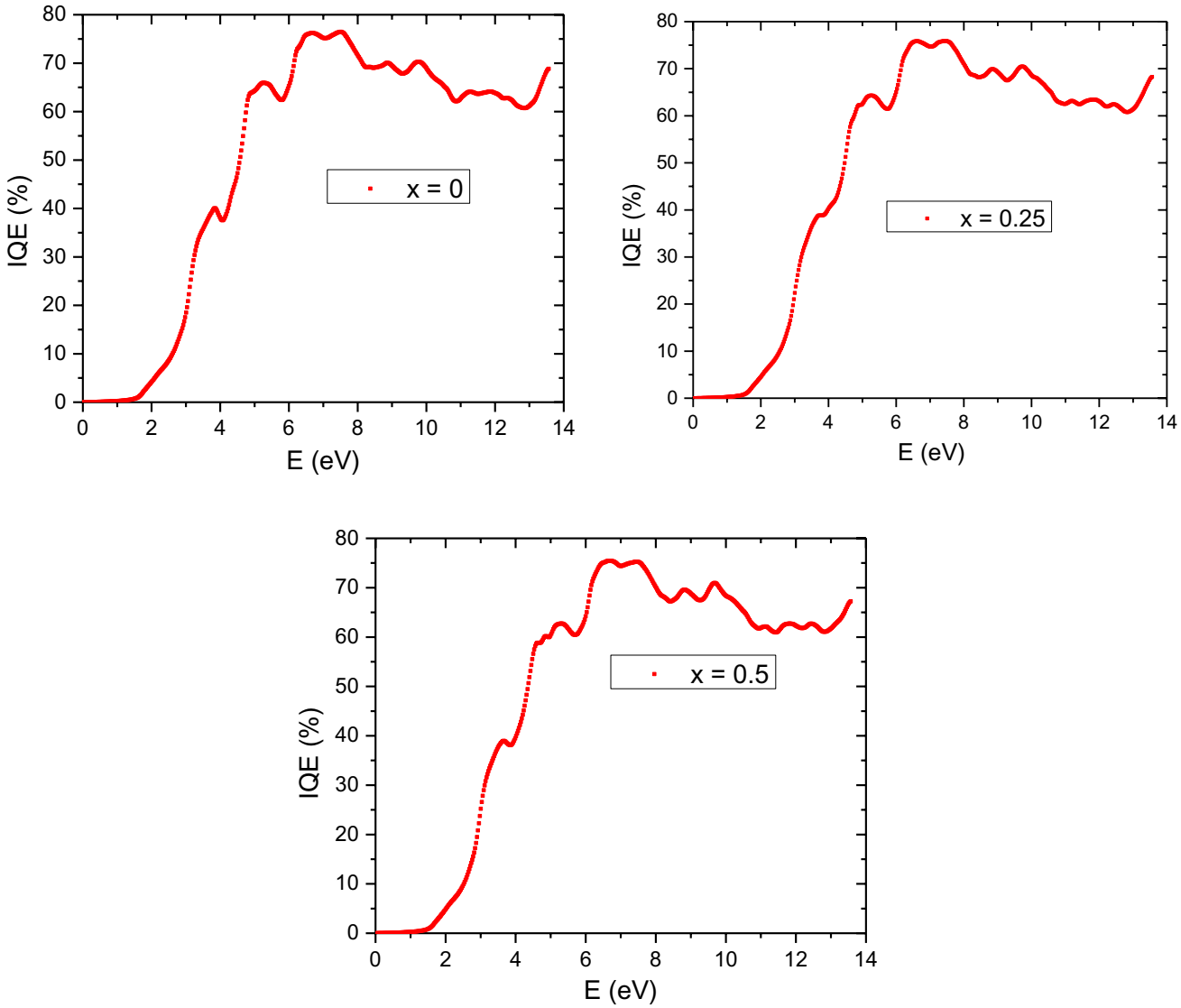

Fig. 9 Internal quantum efficiency of Zn-doping CdTe bulk vs. of photon energy

study for the infrared and visible range of solar radiation. This kind of materials active in infrared and visible radiation are generally suitable for endemic photovoltaic devices [34]. However, the reflectivity of $Cd_{1-x}Zn_xTe$ bulk display in Fig. 7b. The R curve for three materials starts approximately from the same point 0.189%.

Figure 8 display the external quantum efficiency EQE vs. photon energy of $Cd_{1-x}Zn_xTe$ bulk. The maximum of EQE of Zn doping CdTe is equal to 44%, 43.79% and 43.71% when the light energy is larger than the band gap 1.708 eV, 1.673 eV and 1.642 eV for CdTe, $Cd_{0.75}Zn_{0.25}Te$ and $Cd_{0.5}Zn_{0.5}Te$ bulk, respectively.

Figure 9 displays the internal quantum efficiency IQE vs. photon energy of Zn doping CdTe bulk. The maximum of IQE is higher than 76.35%, 75.88% and 75.11% when the light energy is greater than the band gap 1.708 eV, 1.673 eV and 1.642 eV for CdTe, $Cd_{0.75}Zn_{0.25}Te$ and $Cd_{0.5}Zn_{0.5}Te$ bulk respectively.

4 Conclusion

The CdTe thin film was successfully studied using density functional theory (DFT) calculation. The direct band gap is evaluated as 1.58 eV with high-absorption 100 10^4 cm^{-1} for the visible solar spectrum. Internal quantum efficiency (IQE) and external quantum efficiency (EQE) are determined. We found good results compared to those found experimentally and theoretically.

Regarding $Cd_{1-x}Zn_xTe$ bulk we demonstrated that Zn-doped CdTe bluk decreased the bandgap to an optimal value, which led to the fact that $Cd_{1-x}Zn_xTe$ bulk can

become a promising candidate for work in solar cells application. The obtained results of studies of the electronic properties of these materials were compared with existing experimental data and other theoretical calculations. The absorption spectra show that with an increase in the Zn concentration, the absorption edges shift towards shorter waves. Internal quantum efficiency (IQE) and external quantum efficiency (EQE) of Zn doping CdTe bulk are investigated.

Author contributions GK and RM: Conceptualization, methodology, software, investigation, validation, formal analysis, formal analysis, no funding acquisition, writing—original draft preparation, writing—reviewing and editing, supervision, project administration.

Funding No funding received.

Availability of data and materials The data that support the findings of this study are available from the corresponding author upon reasonable request.

Declarations

Conflict of interest No conflict interest.

Ethical approval No applicable.

References

1. C. Liu, B. Wu, R. Cheung, Advanced algorithm for MPPT control of photovoltaic systems. In: Canadian Solar Buildings Conference, Montreal. J. Power Energy Eng. **8**, 20–24 (2004)
2. S. Kasap, P. Capper, *Handbook Springer of Electronic and Photonic Materials* (Springer Science & Business Media, New York, 2006)
3. M. Saliba, L. Etgar, Current density mismatch in perovskite solar cells. ACS Energy Lett. **5**(9), 2886–2888 (2020)
4. D.N. Congreve, J. Lee, N.J. Thompson, E. Hontz, S.R. Yost, P.D. Reusswig, M.A. Baldo, External quantum efficiency above 100% in a singlet-exciton-fission-based organic photovoltaic cell. Science **340**(6130), 334–337 (2013)
5. E. Matioli, C. Neufeld, M. Iza, S.C. Cruz, A.A. Al-Heji, X. Chen, C. Weisbuch, High internal and external quantum efficiency InGaN/GaN solar cells. Appl. Phys. Lett. **98**(2), 021102 (2011)
6. M. Shatalov, W. Sun, A. Lunev, X. Hu, A. Dobrinsky, Y. Bilenko, M. Wraback, AlGaN deep-ultraviolet light-emitting diodes with external quantum efficiency above 10%. Appl. Phys. Express **5**(8), 082101 (2012)
7. H. Choi, S.J. Ko, Y. Choi, P. Joo, T. Kim, B.R. Lee, J.Y. Kim, Versatile surface plasmon resonance of carbon-dot-supported silver nanoparticles in polymer optoelectronic devices. Nat. Photonics **7**(9), 732–738 (2013)
8. G. Kadim, R. Masrour, A. Jabar, Ferroelectric, quantum efficiency and photovoltaic properties in perovskite $BiFeO_3$ thin films: first principle calculations and Monte Carlo study. Int. J. Energy Res. **45**, 9961–9969 (2021)
9. S. Abdellatif, K. Kirah, H. Ghali, W. Anis, A comparison between Si and GaAs nanowire-based photovoltaic devices. In: *SPIE Smart Nano-Micro Materials and Devices Symposium*, Melbourne, Australia, 5–7 December 2011. Proc. SPIE 8204, 820412 (2011). https://doi.org/10.1117/12.921047
10. K. Yao, H. Zhong, Z. Liu, M. Xiong, S. Leng, J. Zhang, A.K.Y. Jen, Plasmonic metal nanoparticles with core–bishell structure for high-performance organic and perovskite solar cells. ACS Nano **13**(5), 5397–5409 (2019)
11. C. Ma, D. Zheng, D. Demaille, B. Gallas, C. Schwob, T. Pauporté, L. Coolen, Light management in highly textured perovskite solar cells: From full-device ellipsometry characterization to optical modelling for quantum efficiency optimization. Sol. Energy Mater. Sol. Cells **230**, 111144 (2021)
12. T. Gokmen, O. Gunawan, D.B. Mitzi, Minority carrier diffusion length extraction in Cu_2ZnSn (Se, S)$_4$ solar cells. J. Appl. Phys. **114**(11), 114511 (2013)
13. A.M. Karmalawi, D.A. Rayan, M.M. Rashad, Establishment and evaluation of photovoltaic quantum efficiency system at central metallurgical research and development institute. Optik **217**, 164931 (2020)
14. R. Fan, Z. Huai, Y. Sun, X. Li, G. Fu, S. Huang, S. Yang, Enhanced performance of polymer solar cells based on PTB7-Th: PC 71 BM by doping with 1-bromo-4 nitrobenzene. J. Mater. Chem. C **5**(42), 10985–10990 (2017)
15. G.M. Wilson, M. Al-Jassim, W.K. Metzger, S.W. Glunz, P. Verlinden, G. Xiong et al., The 2020 photovoltaic technologies roadmap. J. Phys. D Appl. Phys. **53**(49), 493001 (2020)
16. D.J. Feldman, R.M. Margolis, The economics of residential solar panel installations for customers on tiered rate plans. Open J. Bus. Manag. **7**, 1–74 (2019)
17. K.N. Nithyayini, S.K. Ramasesha, Fabrication of semi-transparent photovoltaic cell by a cost-effective technique. Metall. Mater. Trans. E **2**(3), 157–163 (2015)
18. A. Morales-Acevedo, Thin film CdS/CdTe solar cells: research perspectives. Sol. Energy **80**(6), 675–681 (2006)
19. C. Polop, I. Mora-Sero, C. Munuera, J.G. de Andres, V. Munoz-Sanjose, C. Ocal, Twin coarsening in CdTe (1 1 1) films grown on GaAs (1 0 0). Acta Mater. **54**(16), 4285–4291 (2006)
20. K. Shen, Z. Bai, Y. Deng, R. Yang, D. Wang, Q. Li, D. Wang, High efficiency CdTe solar cells with a through-thickness polycrystalline CdTe thin film. RSC Adv. **6**(57), 52326–52333 (2016)
21. J.M. Burst, J.N. Duenow, D.S. Albin, E. Colegrove, M.O. Reese, J.A. Aguiar, W.K. Metzger, CdTe solar cells with open-circuit voltage breaking the 1 V barrier. Nat. Energy **1**(3), 1–8 (2016)
22. R. Gul, A. Bolotnikov, H.K. Kim, R. Rodriguez, K. Keeter, Z. Li, R.B. James, Point defects in CdZnTe crystals grown by different techniques. J. Electron. Mater. **40**(3), 274 (2011)
23. U.N. Roy, G.S. Camarda, Y. Cui, R.B. James, Advances in CdZnTeSe for radiation detector applications. Radiation **1**(2), 123–130 (2021)
24. S. Lalitha, S.Z. Karazhanov, P. Ravindran, S. Senthilarasu, R. Sathyamoorthy, J. Janabergenov, Electronic structure, structural and optical properties of thermally evaporated CdTe thin films. Physica B **387**(1–2), 227–238 (2007)
25. G. Kadim, R. Masrour, A. Jabar, Magnetocaloric effect, electronic and magnetic properties of $Ba_{1-x}Sr_xFeO_3$ barium-strontium ferrites: Monte Carlo simulations and comparative study between TB-mBJ and GGA+ U. Mater. Today Commun. **26**, 102071–102078 (2021)
26. G. Kadim, R. Masrour, A. Jabar, A comparative study between GGA, WC-GGA, TB-mBJ and GGA+ U on magnetocaloric effect, electronic, optic and magnetic properties of $BaMnS_2$ compound: DFT calculation and Monte Carlo simulation. Phys. Scr. **96**, 045804 (2021)

27. A.D. Becke, M.R. Roussel, Exchange holes in inhomogeneous systems: a coordinate-space model. Phys. Rev. A **39**, 3761–3767 (1989)
28. H. Wang, Y. Zheng, M.Q. Cai, H. Huang, H.L. Chan, First-principles study on the electronic and optical properties of $BiFeO_3$. Solid State Commun. **149**(15–16), 641–644 (2009)
29. D.E. Swanson, J.R. Sites, W.S. Sampath, Co-sublimation of $CdSe_xTe_{1-x}$ layers for CdTe solar cells. Sol. Energy Mater. Sol. Cells **159**, 389–394 (2017)
30. A. Hendi, R. Alkhraif, H. Alshehri, F. AlKallas, M. Almoneef, A. Laref, K. Ortashi, Photovoltaic performance of thin-film CdTe for solar cell applications. J. Nanofluids **10**(1), 91–97 (2021)
31. M.A. Sayeed, H.K. Rouf, Effect of Zn-doping on the structural, optical and electrical properties of thermally vacuum evaporated CdTe thin films. Surf. Interfaces **23**, 100968 (2021)
32. A.H. Munshi, J. Kephart, A. Abbas, J. Raguse, J.N. Beaudry, K. Barth, W. Sampath, Polycrystalline CdSeTe/CdTe absorber cells with 28 mA/cm 2 short-circuit current. IEEE J. Photovolt. **8**(1), 310–314 (2017)
33. S.H. Park, A. Roy, S. Beaupre, S. Cho, N. Coates, J.S. Moon, A.J. Heeger, Bulk heterojunction solar cells with internal quantum efficiency approaching 100%. Nat. Photonics **3**(5), 297–302 (2009)
34. M.D. Wisser, S. Fischer, P.C. Maurer, N.D. Bronstein, S. Chu, A.P. Alivisatos, J.A. Dionne, Enhancing quantum yield via local symmetry distortion in lanthanide-based upconverting nanoparticles. ACS Photonics **3**(8), 1523–1530 (2016)